Health vulnerability related to climate extremes in Amazonia and the Brazilian Northeast

Gilvan Guedes[1], Pollyanne Silva[2], Kenya Noronha[3], Lara Andrade[2], and Claudio Silva[2]

[1] Demography Department, Av. Antonio Carlos 6627, Universidade Federal de Minas Gerais, Belo Horizonte, Brazil (1st author's e-mail: gilvan@gilvanguedes.com)
[2] Climatic and Atmospheric Sciences Department, Av. Senador Salgado Filho, 3000, Universidade Federal do Rio Grande do Norte, Candelaria, Natal, RN, Brazil (2nd author's: pollyanne.es@gmail.com, 3rd author's: lara@ccet.urfn.br and 5th author's: claudiomoises@ccet.ufrn.br)
[3] Economics Department, Av. Antonio Carlos, 6627, Universidade Federal de Minas Gerais, Belo Horizonte, Brazil (4th author's: knoronha@cedeplar.ufmg.br)

Abstract. The Brazilian Amazon and the Brazilian Northeast are the two regions with the highest levels of vulnerability to climate change in the country. While the first is characterized by the largest rainforest in the world and has a very hot and humid climate, the second hosts one of the largest deserts in the globe. Because of the very low latitudes, these regions are subject to very high temperatures and are susceptible to many tropical diseases, such as vector-borne (dengue, malaria, yellow fever), water-borne, and gastrointestinal diseases. These diseases are very sensitive to particular climate conditions, such as increase in temperature trend and precipitation concentration. This paper develops a multidimensional index of health vulnerability to climate extremes in Amazonia and the Brazilian Northeast applying the Alkire-Foster method. Vulnerability was conceptualized as represented by three components: risk (proxied by 7 extreme indices based on temperature and precipitation data from the ClimDex project), susceptibility (proxied by socioeconomic and demographic indicators, combining income, education and young and elderly dependency ratios), and adaptive capacity (proxied by sanitation and urbanization variables). Once defined, the index was decomposed by region and levels of climate-sensitive health indicators (infectious and parasitic disease rates) to understand how dimensions of vulnerability correlates with different levels of disease prevalent across regions. Results suggest that 28% of Amazonian regions were deprived in a least 25% of the variables used to create the index, against 8% in the Northeast. The level of health vulnerability varies significantly when homogenous climate zones are taken into account.
Keywords: Extreme Weather, Health Vulnerability, Brazilian Amazonia, Brazilian Northeast, Multidimensional Index.

1 Introduction

Population vulnerability is a multidimensional concept that depends on the society's exposure to adverse conditions defined by the context such as climatic and environmental conditions, sociodemographic and health factors [3, 29]. Vulnerability severity is affected by the interplay between extreme climate events, sociodemographic susceptibility and adaptive capacity of the society [4, 34]. In the short and medium-term, the population vulnerability can be mitigated by public policies such as poverty alleviation, improvements in household infrastructure and access to adequate healthcare services. Climate risks, on the other hand,

require long-term public policies that involve multiple strategies and different actors, both nationally and internationally [40, 33, 10]. They demand structural changes in economic production and human occupation that are not easy to meet. All these changes involve important trade-offs insofar as environmentally sustainable production and consumption may lead to both family and society wealth losses [11, 40, 47].

The most common climate risks, expressed by extreme weather events, are floods, prolonged droughts, gusts, tornadoes, heat waves, and cold waves. These events can cause fatalities, change people's daily lives, impact the economy, and cause infrastructure damage [24]. Extreme climate events can also accelerate the development of pathogens and disease vectors [8, 7, 5]. For example, increasing temperatures may accelerate the life cycle of parasites (e.g malaria) while precipitation volume may contribute to vector propagation [2, 30]. Thus, the occurrence of extreme events can directly affect human health by causing deaths, physical injuries, illness, or mental health problems. In 2009, for instance, 48 deaths were recorded in the Brazilian Northeast (NEB) due to excessive rainfall and consequent landslides [25]. It is important to notice that the severity of health impacts due to extreme climate events depend on the quality of the infrastructure or the degree of adaptive capacity of each society [44, 41].

The intensity and frequency of climate events can be amplified by the climate changes that stem either from natural or anthropogenic factors [49, 22, 43]. Climate interactions with ecosystems, water, biodiversity and changes in land use can lead to environmental degradation, affecting both availability and quality of food and water [28]. Water shortage can aggravate the incidence of infectious diseases due to hygiene conditions and access to drinking water. Empirical evidence has shown that long periods of drought have increased the number of dengue cases due to inadequate water storage [3, 45]. During the 1980s and 1990s, the NEB was affected by prolonged droughts that intensified the human migratory flows from rural to urban areas. As a result, the Northeastern major cities witnessed an increase in visceral leishmaniosis registers [6].

Recently, droughts, floods, cold and heat waves were recorded in different regions of Brazil, such as the drought that hit the South of Brazil in 2008 [24] and the water crisis due to the precipitation deficit in So Paulo in 2014 [26]. The Amazon (AMZ) and NEB regions, in particular, have experienced the most intense and frequent extreme weather events in the country, with periods of torrential rainfall and severe droughts. These events are often responsible for endemic diseases, which intensify the vulnerability of their local population [48].

The AMZ is characterized by a hot and humid climate that is related to meteorological systems at different scales, modulated by ocean-atmosphere mechanisms. These mechanisms cause total rainfall to sit above or below the cl imatological average, producing extremely humid or dry days[39, 38, 43, 9]. In recent years, the region has experienced alternate periods of heavy rainfall and severe droughts. The 2009, 2011, 2012 and 2014 floods displaced thousands of families, interdicted highways, isolated municipalities and increased the incidence of climate-sensitive diseases such as leptospirosis, diarrhea, typhoid fever and dermatitis [23, 23, 25, 27, 51, 46, 16, 15]. The 2005 and 2010 droughts left small riverside communities without sufficient water, affected their fishing activities and increased the incidence of diseases, mainly malaria and dengue that accounted for 56% of morbidities in the region [35, 18, 26].

The NEB, by its turn, is characterized by high climate variability due to physiographic factors and atmospheric systems of different scales [32, 31]. Among the Brazilian regions, the

NEB presents the lowest water availability particularly in the semiarid areas [25]. It has a noticeable inter-annual variation of precipitation, alternating extremely dry and extremely rainy years [21, 13]. Droughts are part of the natural climate variability in the region and recurrently affect the population, especially the most vulnerable inhabitants in the semiarid. Constant water shortages affect the agricultural sector, increasing the risks of food insecurity and worsening the socioeconomic conditions as the region is highly dependent on the family farming [20, 14, 42]. Between 2012 and 2016, NEB experienced the worst drought of the last 50 years that affected 1,100 cities. Besides, important economic sectors, such as agriculture and livestock, suffered significant losses. The depletion of important water sources has triggered a number of hazardous conditions, including the contamination of the water sources, which contributed to increase in the incidence of infectious and parasitic diseases [37]. On the other hand, the the major cities suffered from heavy rainfall episodes. These events associated with poor infrastructure and unplanned urban growth resulted in severe flooding with adverse consequences to the population health [17, 36].

The aim of this paper is to estimate a climate extreme vulnerability index (CEVI) for the AMZ and the NEB taking into account three different dimensions: **risk**, **susceptibility**, and **adaptive capacity**. In addition, we evaluate the relationship between health and each CEVI dimension. Population health conditions were proxied by climate-sensitive infectious and parasitic diseases due to the high incidence of these conditions in both Brazilian regions. For the best of our knowledge, there are only a few studies that evaluate climate, demographic and health conditions for these regions. Our main findings indicate the high vulnerability of the NEB and Amazonia due to the high rates of poverty and natural disasters, with important regional differences. Amazonia is more sensitive to adaptive capacity, while in the NEB risk and suceptibility plays a bigger role in explaining the vulnerability of its regions. In terms of the sensitivity of the CEVI to disease incidence, we observe that in both regions the contribution of the risk dimension is higher in areas with higher incidence. But while suceptibility dimension prevails in NEB in areas of low incidence and the adaptive capacity takes place where incidence is high, in Amazonia adaptive capacity is always the major contributor to vulnerability, regarless of incidence level.

2 Data

The object of this study comprises two Brazilian regions: NEB and AMZ. The political-administrative division follows the Brazilian Institute of Geography and Statistics (IBGE) definition. IBGE defines 27 and 35 mesoregions in the AMZ and NEB, respectively. The meteorological data used in this study came from a joint project between the University of Texas (USA) and the Federal University of Esprito Santo (Brazil) and are available at https://utexas.box.com /Xavier-etal-IJOC-DATA. The methodology for the extraction of this database is described by Xavier et al. [50], which provides the following meteorological variables: precipitation, wind, minimum and maximum temperature, relative humidity and evapotranspiration. These variables are organized in a regular grid of $0.25^o \times 0.25^o$ and cover the entire Brazilian territory. A grid point of precipitation and temperature variables was selected to represent each of the 62 mesoregions (Figure 1). The daily measurement comprises a time series from January 1, 1980 to December 31, 2013.

Population health conditions were proxied by climate-sensitive infectious and parasitic diseases such as diarrhea and gastroenteritis, cholera, malaria, dengue, leptospirosis, leishmaniosis and arbovirus. This indicator was derived from administrative health records pro-

vided by the Brazilian Hospital Information System. This information refers to in-patient care received in the Brazilian Public Health Care System (*SUS-Sistema Único de Saúde*), which responds for 66% of the total hospitalizations in the country [19]. The health data were obtained at the mesoregions level of the AMZ and NEB, using the place of residence instead of place of occurrence as the criterion for data selection. Disease counts are based on a 3-year average centered in 2010. The population used to calculate the rates of climate-sensitive diseases as well as the information about demographic, socioeconomic and infrastructure conditions came from the 2010 Demographic Census conducted by IBGE.

Fig. 1. Grid Points for Meteorological Data and State/Region Boundaries of Study Area

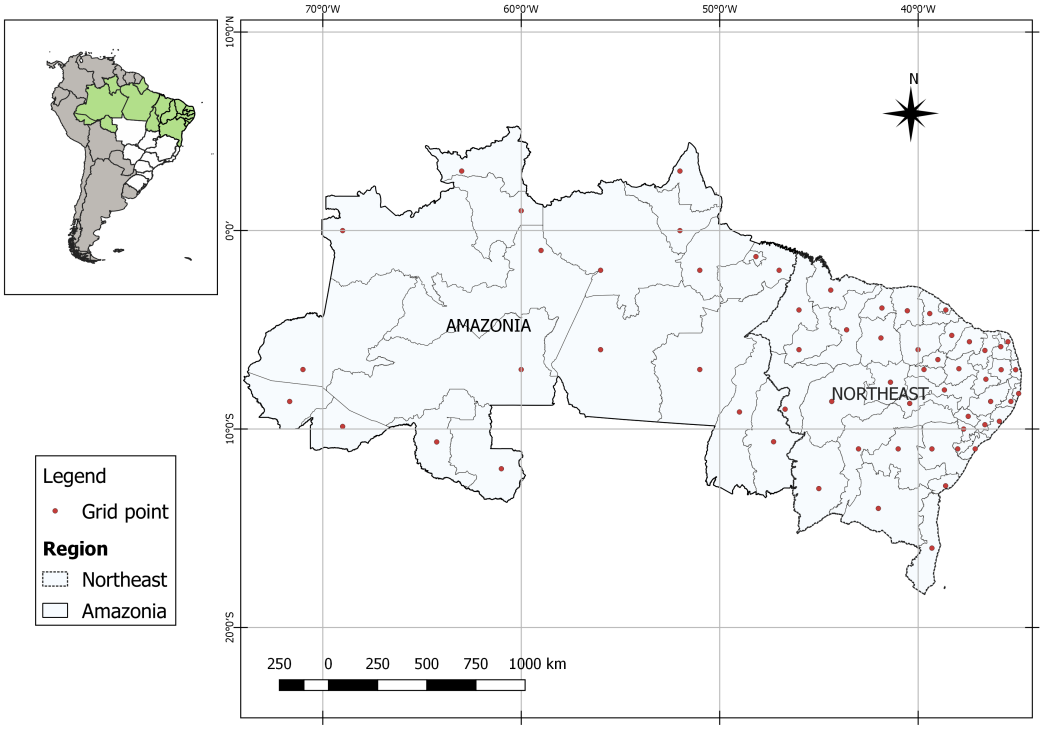

3 Methodology

In order to capture how health correlates with climate and socioeconomic indicators in the Brazilian Northeast and Amazonia, we develop a multidimensional index of health vulnerability to climate extremes (CEVI) applying the Alkire-Foster method [1]. The index was computed at the mesoregion level for the overall study area and by region (NEB and AMZ,

separately). Then, for each of these areas the index was further computed and decomposed by levels of infectious disease incidence.

The CEVI (M_0) is defined by an interaction of two subindices: a censored (multidimensional) deprivation headcount (H) and a censored deprivation intensity (A). We first define the dimensions that constitute vulnerability. In this study we use *risk*, *suceptibility* and *adaptive capacity* as its three main constituents. Then, we elicit the indicators forming each dimension, as shown in Figure 2. To proxy **risk**, we use 5 temperature extreme indices and 2 precipitation extreme indices produced by the Climdex Project [12]: 1) TXx (Monthly maximum value of daily maximum temperature - C^o); 2) TNx (Monthly maximum value of daily minimum temperature - C^o); 3) TX90p (Percentage of days when TX $>$ 90th percentile - warm days); 4) TN90p (Percentage of days when TN $>$ 90th percentile - warm nights); 5) DTR (Daily temperature range: monthly mean difference between TX and TN - C^o); 6) CDD (Maximum number of consecutive days when rainfall $<$1 mm - dry spell); 7) R99p (Annual rainfall that exceeded the 99th percentile in the period from 1980 to 2013 - percentile: extremely wet days in mm). The **suceptibility** dimension was formed by the following indices: 1) regions with proportion of elderly above the 5th quintile of the elderly distribution and below the 1st decile of the average per capita income; 2) regions with proportion of children above the 5th quintile of the children distribution and below the 1st decile of the average per capita income; 3) regions with average per capita income below R\$255.00, and 4) regions with the lowest proportion of literate adults (below the 1st quartile). Finally, the **adaptive capacity** dimension was proxied by 4 indicators: 1) regions with the lowest proportion of households with adequate sewage (below the 1st quartile); 2) regions with the lowest proportion of households with adequate water supply (below the 1st quartile); 3) regions with the lowest proportion of households with gargabe collection (below the 1st quartile), and 4) regions with the lowest levels of urbanization (below the 1st quartile). Finally, we assinged weights for each for dimension equally, that is, 1/3. Since the risk dimension has more indicators, weights vary by indicator whitin dimension, preserving the dimensional weighting scheme. This weigthing structure is shown in Table 1.

This value represents 1/4 of the Brazilian minimum salary by 2010, the year corresponding of most of the data collected.

Fig. 2. Dimensions and Indications withing Dimensions used to create the Climate Extreme Vulnerability Index - CEVI

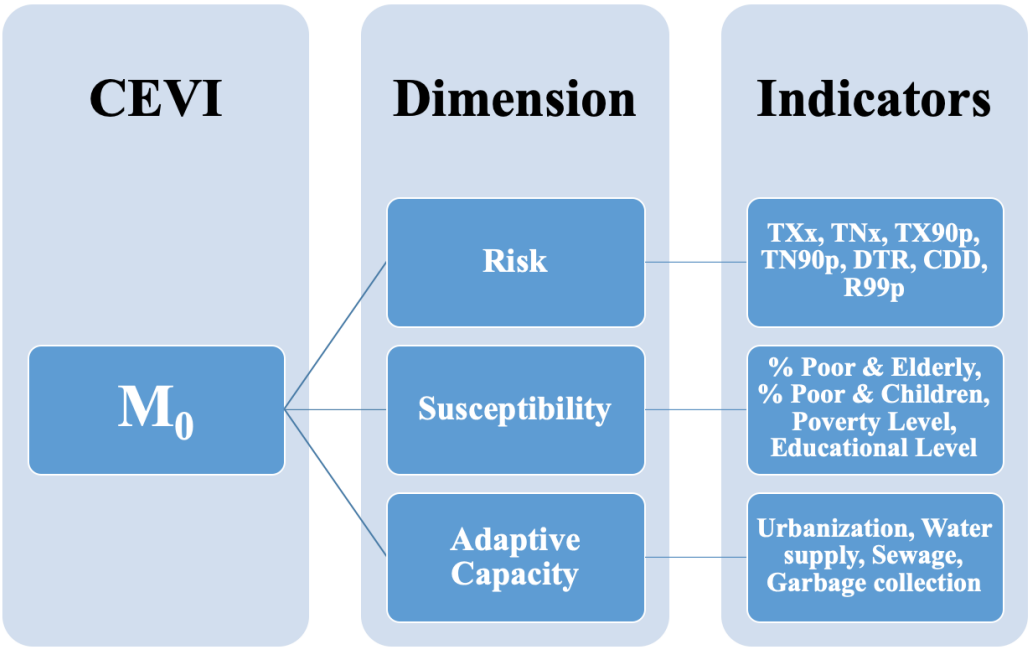

Table 1. Cut-offs and weights attributed to each indicator of CEVI

Dimension	**Indicator**	**Deprivation Cut-off**	**Weight**
Risk	Monthly max value of daily max temperature	4th quartile	0.0333
	Montlhy max value of daily min temperature	4th quartile	0.0333
	Percentage of days when max temperature sit above 90th pct	4th quartile	0.0333
	Percentage of days when min temperature sit above 90th pct	4th quartile	0.0333
	Daily temperature range	4th quartile	0.0333
	Max number of consecutive days when rainfall $< 1mm$	4th quartile	0.0833
	Annual rainfall that exceeded the 99th pct	4th quartile	0.0833
Suceptibility	High proportion of elderly and poor	5th quintile (eldery) & 1st quintile (avg per capita income)	0.0833
	High proportion of children and poor	5th quintile (children) & 1st quintile (avg per capita income)	0.0833
	High proportion of poor	Average per capita income $< R\$255.00$	0.0833
	Lower proportion of literate adults	1st quartile	0.0833
Adaptive Capacity	Lower proportion of household with adequate sewage	1st quartile	0.0833
	Lower proportion of household with adequate water supply	1st quartile	0.0833
	Lower proportion of household with garbage collection	1st quartile	0.0833
	Lower urbanization rate	1st quartile	0.0833

After defining indicators and linking them to dimensions, and after assinging proper weights, the next step in the CEVI construction is to define the number of indices (or dimensions) a mesoregion needs to be simultaneously deprived to be considered as vulnerable. Following Alkire and Foster [1], we estimate different proportions of indicators in which each region is classified as deprived in order to analyse where the curve of the adjusted headcount ratio (M_0) stabilizes. We used overall and regional dominance analysis (not shown here) to define the 25% point as the vulnerability cut-off since it represents the point in which there is a disturbance in the vulnerability trend among regions. Up to this point adjusted headcount (H) and the CEVI were dropping fast (between 35% and 50%), and after it the decrease in deprivation rates reduced.

The second step is the estimation of the breadth of vulnerability experienced by each vulnerable region. This step is crucial to adjust the unadjusted CEVI level (H) to its intensity (A). It represents the share of possible deprivations experienced by a multidimensionally vulnerable region. The adjusted CEVI (M_0) is also called adjusted headcount ratio. It measures the proportion of regions that are classified as simultaneously deprived on at least 25% of the indicators weighted by its intensity.

3.1 Index Decomposition by Region

If the entire study area, y (of size n) is divided into two subgroups y_1 (of size n_1) and y_2 (of size n_2), then M_0 can be decomposed as

$$M_0(y) = \frac{n_1}{n} * M_0(y_1) + \frac{n_2}{n} * M_0(y_2) \tag{1}$$

The contribution of subgroup i to the overall adjusted CEVI (M_0) is:

$$\frac{n_i}{n} * \left[\frac{M_0(y_i)}{M_0(y)}\right], \text{ for } i = 1, 2 \tag{2}$$

3.2 Index Decomposition by Dimension or Indicator

If the censored headcount of indicator d is denoted by H_d, then the adjusted CEVI can be expressed as

$$M_0(y) = \sum_d \left(\frac{w_d}{D}\right) * H_d \tag{3}$$

where w_d is the weight attached to dimension d. If decomposition is to be made by indicator, just read d is the indicator. The contribution of dimension d to the overall CEVI is

$$\left(\frac{w_d}{D}\right) * \left[\frac{H_d}{M_0(y)}\right], \text{ for all } d \tag{4}$$

A 45% cut-off point was another break-up point in the curve, but it would produce a very small number of multidimensional deprived regions (only 6), since the criterion for deprivation would be to severe.

4 Results

Table 2 presents descriptive measures of all indicators used to create the CEVI. We observe important differences between unidimensionally (uncensored) deprived and non-deprived mesoregions, with differences more pronounced in AMZ than in NEB. Deprived regions have on average higher proportion of warm days and nights, higher daily temperature, dry spell and extremely wet days compared to the non-deprived regions. Overall, risk indicators are slightly worse for deprived regions in AMZ than in NEB. In terms of suceptibility, AMZ has a higher proportion of deprived regions and because it is the youngest region in the country it has a higher proportion of areas with more children and poor individuals relative to NEB. The proportion of literate adults is also lower in the deprived areas, especially in the AMZ. The larger regional differences, however, is observed in the adaptive capacity dimension, with the AMZ showing the worse levels of overall sanitation conditions, especially among the deprived areas.

Table 2. Descriptive Measures of Indicators used in the Multidimensional Index of Health Vulnerability to Climate Extremes in Amazonia and in the Brazilian Northeast

Indicator	**Total**			**Northeast**			**North**		
	Sample	Not Dep	Deprived	Sample	Not Dep	Deprived	Sample	Not Dep	Deprived
Risk									
Monthly max value of daily max temperature	36.7	35.9	38.9	36.6	35.5	38.9	36.8	36.6	39.8
Monthly max value of daily min temperature	25.0	24.6	26.2	24.9	24.4	26.2	25.0	24.9	26.1
Percentage of days when max temperature sit above 90th pct	16.6	12.8	28.8	15.0	12.5	30.0	20.1	13.7	27.9
Percentage of days when min temperature sit above 90th pct	16.8	12.1	31.4	14.7	12.3	29.4	21.1	11.6	32.7
Daily temperature range	9.9	9.4	11.8	10.1	9.3	11.9	9.6	9.4	11.2
Max number of consecutive days when rainfall < 1 mm	51.6	34.4	105.6	62.7	41.8	104.7	28.3	23.6	117.7
Annual rainfall that exceeded the 99th pct	118.9	82.6	232.6	94.3	76.0	203.9	170.4	103.8	251.8
Suceptibility									
Proportion of elderly and poor*	100.0	92.3	9.7	100.0	88.1	11.9	100.0	95.0	5.0
Proportion of children and poor*	100.0	83.9	16.1	100.0	88.1	11.9	100.0	75.0	25.0
Proportion of poor	100.0	88.7	11.3	100.0	92.9	7.1	100.0	80.0	20.0
Proportion of literate adults	65.1	66.9	59.8	66.0	67.1	61.2	63.2	66.4	58.5
Adaptative Capacity									
Proportion of hh with adequate sewage	80.3	86.2	63.3	83.3	86.4	69.9	74.1	85.7	56.8
Proportion of hh with adequate water supply	67.0	75.1	44.0	73.6	74.9	56.8	53.3	76.0	41.0
Proportion of hh with gargabe collection	68.5	74.5	51.4	69.2	72.8	51.3	67.0	79.8	51.4
Lower urbanization rate	67.4	72.5	52.6	67.2	71.0	53.2	67.8	76.3	51.9

Note: * represents the proportion of mesoregions with the attribute.

Table 3 performs the sensitivity analysis of multidimensional vulnerability by varying cutoff levels. Since we have 15 indicators, our defined our cutoff point, k, as the proportion of the counting vector, $c(i)$, as $k = \frac{c(i)}{\sum_i i}$, where i stands for indicator. We varied k from 10% to 100% to study the curve formed by H and M_0 (our CEVI). As explained in Section 3, with the 25% cut-off point (shown in bold in Table 3), we found that 32.3% of all regions (23.8% in NEB and 50.0% in AMZ) were vulnerable simultaneously on at least 25% of the indicators used in CEVI. If we take the deprivation intensity into account, vulnerability in the region was 14.9%, 10.0% and 25.3% for the overall study region, NEB and AMZ, respectively. All subsequence analyses use the 25% criterion to establish the lower bound of simultaneous deprivation for a region to be considered vulnerable.

Table 3. Censored Headcount, Vulnerability Intensity and Intensity Adjusted Multidimentional Index according to varying Cut-off Levels for the Deprivation Counting Vector

Cut-off	**Censored Headcount**			**Vulnerability Intensity**			**Multidimensional Index**		
(%)	Sample	Northeast	North	Sample	Northeast	North	Sample	Northeast	North
10	0.694	0.643	0.800	0.297	0.254	0.368	0.206	0.163	0.294
15	0.516	0.476	0.600	0.359	0.304	0.450	0.185	0.145	0.270
20	0.403	0.333	0.550	0.415	0.365	0.477	0.167	0.122	0.263
25	**0.323**	**0.238**	**0.500**	0.463	0.422	0.505	**0.149**	**0.100**	**0.253**
30	0.290	0.214	0.450	0.484	0.439	0.530	0.141	0.094	0.238
35	0.258	0.190	0.400	0.504	0.452	0.556	0.130	0.086	0.223
40	0.210	0.143	0.350	0.538	0.483	0.586	0.113	0.069	0.205
45	0.145	0.048	0.350	0.598	0.642	0.586	0.087	0.031	0.205
50	0.113	0.048	0.250	0.640	0.642	0.640	0.072	0.031	0.160
55	0.097	0.048	0.200	0.664	0.642	0.675	0.064	0.031	0.135
60	0.097	0.048	0.200	0.664	0.642	0.675	0.064	0.031	0.135
65	0.081	0.024	0.200	0.670	0.650	0.675	0.054	0.015	0.135
70	0.000	0.000	0.000	0.000	0.000	0.000	0.000	0.000	0.000
75	0.000	0.000	0.000	0.000	0.000	0.000	0.000	0.000	0.000
80	0.000	0.000	0.000	0.000	0.000	0.000	0.000	0.000	0.000
85	0.000	0.000	0.000	0.000	0.000	0.000	0.000	0.000	0.000
90	0.000	0.000	0.000	0.000	0.000	0.000	0.000	0.000	0.000
95	0.000	0.000	0.000	0.000	0.000	0.000	0.000	0.000	0.000
100	0.000	0.000	0.000	0.000	0.000	0.000	0.000	0.000	0.000

Table 4 shows the proportion of regions deprived in each indicator used to create the CEVI. In the first three columns, proportions refer to unidimensional (uncensored) deprivations for each indicator. In the last three columns, proportions of deprivated regions are censored to those who are simultaneously deprived in that particular indicator and are deprived in at least 25% of indicators. Thus, the smaller the difference between uncensored and censored headcounts for the indicator, the more persistent (or structural) vulnerability is for a region. Results show that the smaller average variation occurs in the *suceptibility* dimension, followed by *adaptive capacity*. Between regions, the smallest difference is observed in the AMZ suggesting its highly and persistent vulnerability, both unidimensionally and multidimensionally.

Table 4. Uncensored and Censored (Cut-off=25%) Headcount by Indicator and Region

Indicator	Uncensored Headcount			Censored Headcount		
	Sample	Northeast	North	Sample	Northeast	North
Risk						
R1	24.2	33.3	5.0	11.3	16.7	0.0
R2	24.2	28.6	15.0	9.7	9.5	10.0
R3	24.2	14.3	45.0	12.9	4.8	30.0
R4	24.2	14.3	45.0	9.7	2.4	25.0
R5	24.2	31.0	10.0	9.7	11.9	5.0
R6	24.2	33.3	5.0	8.1	11.9	0.0
R7	24.2	14.3	45.0	9.7	2.4	25.0
Suceptibility						
S1	9.7	11.9	5.0	8.1	9.5	5.0
S2	16.1	11.9	25.0	14.5	9.5	25.0
S3	11.3	7.1	20.0	11.3	7.1	20.0
S4	25.8	19.0	40.0	24.2	16.7	40.0
Adaptative Capacity						
AC1	25.8	19.0	40.0	17.7	9.5	35.0
AC2	25.8	7.1	65.0	17.7	4.8	45.0
AC3	25.8	16.7	45.0	24.2	14.3	45.0
AC4	25.8	21.4	35.0	22.6	16.7	35.0

Note: R1 = Monthly max value of daily max temperature, R2 = Monthly max value of daily min temperature, R3 = Percentage of days when max temperature sit above 90th pct, R4 = Percentage of days when min temperature sit above 90th pct, R5 = Daily temperature range, R6 = Max number of consecutive days when rainfall $<$ 1mm, R7 = Annual rainfall that exceeded the 99th pct, S1 = Proportion of elderly and poor, S2 = Proportion of children and poor, S3 = Proportion of poor, S4 = Proportion of literate adults, AC1 = Proportion of household with adequate sewage, AC2 = Proportion of household with adequate water supply, AC3 = Proportion of household with garbage collection, AC4 = Urbanization rate.

The decomposition of CEVI shows that *risk* and *adaptive capacity* are the two most important dimensions among regions with high incidence of infectious and parasitic diseases. In regions with low incidence, *suceptibility* explains almost 50% of CEVI, followed by *adaptive capacity*. In these regions, *risk* component is less important, contributing 9.6% against 24.7% in regions with high incidence (Table 3).

These reults reflect the nature of the infectious and parasitic diseases, which are sensitive to climatic conditions and to the local sanitary conditions. To show this, we further decompose CEVI by dimension according to both incidence level and region. Regardless of the region, the contribution of *risk* is higher in areas with higher incidence of infectious and parasitic diseases. However, in NEB *suceptibility* prevails in areas of low incidence (68.2%) and *adaptive capacity* takes place where incidence is high (45.1%). In AMZ, *adaptive capacity* is always the major contributor to vulnerability, regardless of incidence level, corresponding to 48.6% (low incidence) and 58.1% (high incidence) respectively. Findings from Table 3 reflects the low coverage of basic public services in the AMZ compared to the NEB. For

Fig. 3. Dimensional Decomposition of Vulnerability by Levels of Infectious Disease Incidence, Overall and by Region

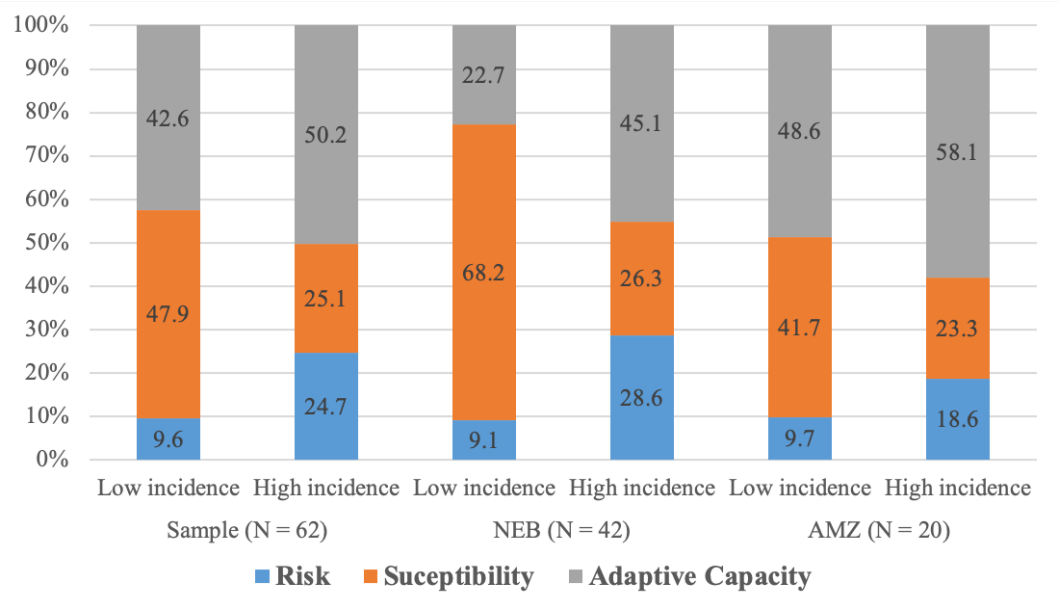

the former, it does not matter if the region has low or high disease incidence, CEVI would always be predominantly explained by the low adaptative capacity of the area.

5 Concluding Remarks

This paper proposed a composite index of vulnerability to climate extreme and sociosanitation conditions for the two more impoverished areas of Brazil: Amazonia and the Northeast. These areas are also the most vulnerable to climate extremes for different reasons: the first host the largest rainforest in the world, while the latter has one of the largest and more impoverished inhabited desert on Earth. Moreover, because both regions lay in very low latitudes, they are prone to high incidence of tropical infectious diseases, causing non-trivial disease burden to their local populations. This paper developed a multidimensional index of health vulnerability to climate extremes in Amazonia and the Brazilian Northeast applying the Alkire-Foster method. Vulnerability was conceptualized as represented by three components: *risk* (proxied by seven extreme indices based on temperature and precipitation data from the ClimDex project), *suceptibility* (proxied by socioeconomic and demographic indicators, combining income, education and young and elderly dependency ratios), and *adaptive capacity* (proxied by sanitation and urbanization variables). Once defined, the index was decomposed by region and levels of climate-sensitive health indicators (infectious and parasitic disease rates) to understand how dimensions of vulnerability correlates with different levels of disease prevalent across regions.

6 Acknowledgements

The authors like to thank CNPq, CAPES, FAPEMIG and Rede Clima/FINEP for the financial support to their research throught FAPEMIG Grant CSA-APQ-00244-12, FAPEMIG Grant CSA-PPM-00305-14, FAPEMIG Grant CSA-APQ-01553-16), CNPq Grant 4837/2012-7, CNPq Grant 472252/2014-3, CNPq Grant 431872/2016-3, CNPq Grant 314392/2018-1), and FINEP/ Rede CLIMA Grant Number 01.13.0353-00).

Bibliography

[1] Alkire, S. and J. Foster (2011). Counting and multidimensional poverty measurement. *Journal of public economics 95*(7-8), 476–487.

[2] Altizer, S., R. S. Ostfeld, P. T. Johnson, S. Kutz, and C. D. Harvell (2013). Climate change and infectious diseases: from evidence to a predictive framework. *science 341*(6145), 514–519.

[3] Barcellos, C., A. M. V. Monteiro, C. Corvalán, H. C. Gurgel, M. S. Carvalho, P. Artaxo, S. Hacon, and V. Ragoni (2009). Mudanças climáticas e ambientais e as doenças infecciosas: cenários e incertezas para o brasil. *Epidemiologia e Serviços de Saúde 18*(3), 285–304.

[4] Cardona, O.-D., M. K. van Aalst, J. Birkmann, M. Fordham, G. McGregor, and R. Mechler (2012). Determinants of risk: exposure and vulnerability.

[5] Confalonieri, U., M. Barata, and D. Marinho (2015). Vulnerabilidade climática no brasil. *Metodologias de estudos de vulnerabilidade à mudança do clima. Rio de Janeiro: Interciência 5*, 25–38.

[6] Confalonieri, U. E. (2003). Variabilidade climática, vulnerabilidade social e saúde no brasil. *Terra livre 1*(20), 193–204.

[7] Confalonieri, U. E. (2010). Mudança climática global e saúde humana no brasil. *Parcerias estratégicas 13*(27), 323–350.

[8] Confalonieri, U. E. (2015). Variabilidade climática, vulnerabilidade social e saúde no brasil. *Terra livre 1*(20), 193–204.

[9] da Silva, P. E., C. M. Santos, M. H. C. Spyrides, L. d. M. B. Andrade, et al. (2019). Análise de índices de extremos climáticos no nordeste e amazônia brasileira para o período entre 1980 a 2013. *Anuário do Instituto de Geociências 42*(2), 137–148.

[10] Darela Filho, J. P., D. M. Lapola, R. R. Torres, and M. C. Lemos (2016). Socio-climatic hotspots in brazil: how do changes driven by the new set of ipcc climatic projections affect their relevance for policy? *Climatic change 136*(3-4), 413–425.

[11] de Sherbinin, A. (2014). Climate change hotspots mapping: what have we learned? *Climatic Change 123*(1), 23–37.

[12] Donat, M., L. Alexander, H. Yang, I. Durre, R. Vose, R. Dunn, K. Willett, E. Aguilar, M. Brunet, J. Caesar, et al. (2013). Updated analyses of temperature and precipitation extreme indices since the beginning of the twentieth century: The hadex2 dataset. *Journal of Geophysical Research: Atmospheres 118*(5), 2098–2118.

[13] Du, H., L. V. Alexander, M. G. Donat, T. Lippmann, A. Srivastava, J. Salinger, A. Kruger, G. Choi, H. S. He, F. Fujibe, et al. (2019). Precipitation from persistent extremes is increasing in most regions and globally. *Geophysical Research Letters 46*(11), 6041–6049.

[14] Eakin, H. C., M. C. Lemos, and D. R. Nelson (2014). Differentiating capacities as a means to sustainable climate change adaptation. *Global Environmental Change 27*, 1–8.

[15] Espinoza, J. C., J. Ronchail, F. Frappart, W. Lavado, W. Santini, and J. L. Guyot (2013). The major floods in the amazonas river and tributaries (western amazon basin) during the 1970–2012 period: A focus on the 2012 flood. *Journal of Hydrometeorology 14*(3), 1000–1008.

[16] Espinoza, J. C., J. Ronchail, J. L. Guyot, C. Junquas, G. Drapeau, J. M. Martinez, W. Santini, P. Vauchel, W. Lavado, J. Ordoñez, et al. (2012). From drought to flooding: understanding the abrupt 2010–11 hydrological annual cycle in the amazonas river and tributaries. *Environmental Research Letters 7*(2), 024008.

[17] Freire, F. G. C., A. M. de Paiva Oliveira, J. E. Sobrinho, R. O. Batista, W. de Oliveira Santos, and H. B. F. Barreto (2013). Estudo das precipitações máximas para o município de mossoró-rn, brasil. *REVISTA BRASILEIRA DE AGRICULTURA IRRIGADA-RBAI 6*(1).

[18] Groisman, P. Y., R. W. Knight, D. R. Easterling, T. R. Karl, G. C. Hegerl, and V. N. Razuvaev (2005). Trends in intense precipitation in the climate record. *Journal of climate 18*(9), 1326–1350.

[19] IBGE (2014). Pesquisa nacional de sade 2013: percepo do estado de sade, estilos de vida e doenas crnicas.

[20] Kayano, M. T., R. V. Andreoli, and R. A. Ferreira de Souza (2013). Relations between enso and the south atlantic sst modes and their effects on the south american rainfall. *International Journal of Climatology 33*(8), 2008–2023.

[21] Kayano, M. T., R. V. Andreoli, and R. A. F. d. Souza (2019). El niño–southern oscillation related teleconnections over south america under distinct atlantic multidecadal oscillation and pacific interdecadal oscillation backgrounds: La niña. *International Journal of Climatology 39*(3), 1359–1372.

[22] Lee, H., S. Park, S. Kim, C. Choi, S. Lee, et al. (2017). The effects of high air temperature and waterlogging on the growth and physiological responses of hot pepper. *Horticultural Science and Technology 35*(1), 69–78.

[23] Marengo, J., C. Nobre, J. Tomasella, M. Cardoso, and M. Oyama (2008). Hydroclimatic and ecological behaviour of the drought of amazonia in 2005. *Philosophical Transactions of the Royal Society B: Biological Sciences 363*(1498), 1773–1778.

[24] MARENGO, J. A. (2009). Mudanças climáticas, condições meteorológicas extremas e eventos climáticos no brasil. *Fundação Brasileira para o Desenvolvimento Sustentável (FBDS). Mudanças climáticas e eventos extremos no Brasil. Disponível em: http://www. fbds. org. br/fbds/IMG/pdf/doc-504. pdf. Acesso em 24*.

[25] Marengo, J. A., L. M. Alves, E. A. Beserra, and F. F. Lacerda (2011). Variabilidade e mudanças climáticas no semiárido brasileiro. *Recursos hídricos em regiões áridas e semiáridas 1*.

[26] Marengo, J. A., L. E. Aragão, P. M. Cox, R. Betts, D. Costa, N. Kaye, L. T. Smith, L. M. Alves, and V. Reis (2016). Impacts of climate extremes in brazil: the development of a web platform for understanding long-term sustainability of ecosystems and human health in amazonia (pulse-brazil). *Bulletin of the American Meteorological Society 97*(8), 1341–1346.

[27] Marengo, J. A., J. Tomasella, W. R. Soares, L. M. Alves, and C. A. Nobre (2012). Extreme climatic events in the amazon basin. *Theoretical and Applied Climatology 107*(1-2), 73–85.

[28] McMichael, A. J. and B. A. Wilcox (2009). Climate change, human health, and integrative research: a transformative imperative.

[29] Menezes, J. A., U. Confalonieri, A. P. Madureira, I. de Brito Duval, R. B. dos Santos, and C. Margonari (2018). Mapping human vulnerability to climate change in the brazilian amazon: the construction of a municipal vulnerability index. *PloS one 13*(2), e0190808.

[30] Mordecai, E. A., K. P. Paaijmans, L. R. Johnson, C. Balzer, T. Ben-Horin, E. de Moor, A. McNally, S. Pawar, S. J. Ryan, T. C. Smith, et al. (2013). Optimal temperature

for malaria transmission is dramatically lower than previously predicted. *Ecology letters 16*(1), 22–30.

[31] Oliveira, P. T. d., C. S. e Silva, and K. Lima (2017). Climatology and trend analysis of extreme precipitation in subregions of northeast brazil. *Theoretical and applied climatology 130*(1-2), 77–90.

[32] Oliveira, P. T. d., C. M. S. e. Silva, and K. C. Lima (2014). Linear trend of occurrence and intensity of heavy rainfall events on northeast brazil. *Atmospheric Science Letters 15*(3), 172–177.

[33] on Climate Change. Working Group II, I. P. (2014). *Climate change 2014: impacts, adaptation, and vulnerability*. IPCC Working Group II.

[34] Oppenheimer, M., M. Campos, R. Warren, J. Birkmann, G. Luber, B. ONeill, and K. Takahashi (2014). Emergent risks and key vulnerabilities climate change 2014: Impacts, adaptation, and vulnerability. part a: Global and sectoral aspects. contribution of working group ii to the fifth assessment report of the intergovernmental panel on climate change ed cb field et al.

[35] Parry, M., M. L. Parry, O. Canziani, J. Palutikof, P. Van der Linden, and C. Hanson (2007). *CONFALONIERI, U. E. C.; MENNE, B. Human health. In: Climate change 2007-impacts, adaptation and vulnerability: Working group II contribution to the fourth assessment report of the IPCC*, Volume 4. Cambridge University Press.

[36] Rosendo, Q., E. Eldan, B. I. de Souza, A. L. Pires, L. P. Dutra Pedrosa, and H. J. Almeida Filgueira (2015). Extreme rainfall and territorial disorder in the construction of risk: A case study in the cabaceiras municipality of paraíba, brazil. *Cuadernos de Geografía-Revista Colombiana de Geografía 24*(2), 189–203.

[37] Rufino, R., R. Gracie, A. Sena, C. M. d. Freitas, and C. Barcellos (2016). Surtos de diarreia na região nordeste do brasil em 2013, segundo a mídia e sistemas de informação de saúde–vigilância de situações climáticas de risco e emergências em saúde. *Ciência & Saúde Coletiva 21*, 777–788.

[38] Santos, C. A. C. d. and V. G. d. Oliveira (2017). Trends in extreme climate indices for pará state, brazil. *Revista Brasileira de Meteorologia 32*(1), 13–24.

[39] Santos, E. B., P. S. Lucio, and C. M. S. e. Silva (2015). Precipitation regionalization of the brazilian amazon. *Atmospheric Science Letters 16*(3), 185–192.

[40] Sena, A., K. L. Ebi, C. Freitas, C. Corvalan, and C. Barcellos (2017). Indicators to measure risk of disaster associated with drought: Implications for the health sector. *PloS one 12*(7), e0181394.

[41] Sena, A., C. Freitas, P. F. Souza, F. Carneiro, T. Alpino, M. Pedroso, C. Corvalan, and C. Barcellos (2018). Drought in the semiarid region of brazil: Exposure, vulnerabilities and health impacts from the perspectives of local actors. *PLoS currents 10*.

[42] Silva, M. A. M. d., M. N. M. de Araújo Frutuoso, S. S. F. B. Rodrigues, and R. J. M. C. Nogueira (2016). Fatores socioambientais influenciados pela seca na conservação da caatinga. *HOLOS 4*, 245–257.

[43] Silva, P. E. d., C. M. Santos e Silva, M. H. C. Spyrides, and L. d. M. B. Andrade (2019). Precipitation and air temperature extremes in the amazon and northeast brazil. *International Journal of Climatology 39*(2), 579–595.

[44] Smith, L. T., L. E. Aragao, C. E. Sabel, and T. Nakaya (2014). Drought impacts on children's respiratory health in the brazilian amazon. *Scientific reports 4*, 3726.

[45] Souza, M., L. Andrade, M. Spyrides, and J. Justino (2018). Bayesian estimates for the mapping of dengue hotspots and estimation of the risk of disease epidemic in northeast brazil. *Urban Climate 26*, 198–211.

[46] Tomasella, J., L. S. Borma, J. A. Marengo, D. A. Rodriguez, L. A. Cuartas, C. A. Nobre, and M. C. Prado (2011). The droughts of 1996–1997 and 2004–2005 in amazonia: hydrological response in the river main-stem. *Hydrological Processes 25*(8), 1228–1242.

[47] Torres, R. R. and J. A. Marengo (2014). Climate change hotspots over south america: from cmip3 to cmip5 multi-model datasets. *Theoretical and applied climatology 117*(3-4), 579–587.

[48] Vianna, J. N. S., M. C. Pereira, L. M. Duarte, and M. E. Wehrmann (2013). O papel das oleaginosas em um cenário de mudanças climáticas no semiárido brasileiro (the role of oilseeds in a climate change scenario in the brazilian semiarid). *Revista Brasileira de Geografia Física 5*(6), 1426–1445.

[49] Wu, C., G. Huang, and H. Yu (2015). Prediction of extreme floods based on cmip5 climate models: a case study in the beijiang river basin, south china. *Hydrology and Earth System Sciences 19*(3), 1385–1399.

[50] Xavier, A. C., C. W. King, and B. R. Scanlon (2016). Daily gridded meteorological variables in brazil (1980–2013). *International Journal of Climatology 36*(6), 2644–2659.

[51] Yoon, J.-H. and N. Zeng (2010). An atlantic influence on amazon rainfall. *Climate Dynamics 34*(2-3), 249–264.